Mesons above T_c*

QCD-TARO Collaboration: Ph. de Forcrand[a], M. García Pérez[b], T. Hashimoto[c], S. Hioki[d], H. Matsufuru[e], O. Miyamura[f], A. Nakamura[g] I.-O. Stamatescu[hi], T. Takaishi[j], and T. Umeda[k]

[a] ETH-Zürich, CH-8092 Zürich, Switzerland
[b] Theory Division, CERN, CH-1211, Geneve 23, Switzerland
[c] Department of Applied Physics, Faculty of Engineering, Fukui University, Fukui 910-8507, Japan
[d] Department of Physics, Tezukayama University, Nara 631-8501, Japan
[e] Yukawa Institute for Theoretical Physics, Kyoto University, Kyoto 606-8502, Japan
[f] Department of Physics, Hiroshima University, Higashi-Hiroshima 739-8526, Japan
[g] Information Media Center, Hiroshima University, Higashi-Hiroshima 739-8521, Japan
[h] Institut für Theoretische Physik, Univ. Heidelberg, D-69120 Heidelberg, Germany
[i] FEST, Schmeilweg 5, D-69118 Heidelberg, Germany
[j] Hiroshima University of Economics, Hiroshima 731-01, Japan
[k] Center for Computational Physics, University of Tsukuba, Tsukuba 305-8577, Japan

We analyse temporal and spatial meson correlators in quenched lattice QCD at $T > 0$. Above T_c we find different (temporal) pole masses and (spatial) screening masses, signals of plasma formation and indication of persisting mesonic excitations.

With increasing temperature we expect the physical picture of QCD to change according to a phase transition where chiral symmetry restoration and deconfinement may simultaneously occur. For model independent non-perturbative results one attempts lattice Monte Carlo studies. Since in the Euclidean formulation the $O(4)$ symmetry is broken at $T > 0$, physics appears different, depending on whether we probe the space ("σ": $\mathbf{x}$) or time ("τ": t) direction: the string tension, e.g., measured from $\sigma\sigma$ Wilson loops does not vanish above T_c, in contrast to the one measured from $\sigma\tau$ loops. *Therefore we need to investigate hadronic correlators with full "space-time" structure, in particular the propagation in the Euclidean time.* The latter, however, poses special problems because of the inherently limited *physical length* of the lattice in the time direction $l_\tau = 1/T$. In the following we shall briefly discuss this question and introduce our procedure. For a more detailed discussion see [1].

1) Lattice problems: Large T can be achieved using small $N_\tau = l_\tau/a$ (a: lattice spacing), however this leads to systematic errors [2]. Moreover, having the t-propagators at only a few points makes it impossible to characterise the unknown structure in the corresponding channels. To obtain a fine t-discretisation and thus detailed t-correlators, while avoiding prohibitively large lattices (we need large spatial size to avoid finite size effects, typically $l_\sigma \sim 3l_\tau$), we use different lattice spacings in space and in time, $a_\sigma/a_\tau = \xi > 1$. For this we employ anisotropic Yang-Mills and fermionic actions [3]:

$$S_{\rm YM} = -\frac{\beta}{3}\left(\frac{1}{\gamma_G}\mathrm{ReTr}\Box_{\sigma\sigma} + \gamma_G \mathrm{ReTr}\Box_{\sigma\tau}\right) \quad (1)$$

$$S_F = \frac{1}{2\kappa_\sigma}\bar{\Psi} W \Psi, \quad (2)$$

$$W = 1 - \kappa_\sigma \textstyle\sum_i \Gamma_i^+ U_i T_i + \gamma_F \Gamma_4^+ U_4 T_4 + \text{"h.c."}) \quad (3)$$

where $\kappa_\sigma^{-1} = 1/2(m_0 + 3 + \gamma_F)$, $\Gamma_\mu^\pm = 1 \pm \gamma_\mu$, T_μ are lattice translation operators and m_0 the bare quark mass. ξ is determined at $T \simeq 0$ by requiring isotropy in the physical distance $F^\sigma(z) = F^\tau(t = \xi z)$ for correlators F ("calibration"). In a quenched simulation at some γ_G, ξ is fixed by the Yang-Mills calibration, then γ_F is tuned to give the same ξ for $T \simeq 0$ hadron correlators. We vary $T = \xi/N_\tau a_\sigma$ by varying N_τ.

*Talk presented by I.-O. Stamatescu.

2) Physical problems: Increasing the temperature is expected to induce significant changes in the structure of the hadrons (see, e.g. [4] for reviews). Two "extreme" pictures are frequently used for the intermediate and the high T regimes, respectively: the weakly interacting meson gas, where we expect the mesons to become effective resonance modes with a small mass shift and width due to the interaction; and the quark-gluon plasma (QGP), where the mesons should eventually disappear and at very high T perturbative effects should dominate. These genuine temperature effects should be reflected in the low energy structure in the mesonic channels. But this structure cannot be observed directly, due to the inherently coarse *energy* resolution $1/l_\tau = T$. Our strategy is the following: we fix at $T = 0$ a mesonic source which gives a large (almost 100%) projection onto the ground state. Then we use this source to determine the changes induced by the temperature on the ground state. For $T > T_c$ we do not have a good justification to use that source as representative of the meson but we assume that it still projects onto the dominant low energy structure in the spectral function. This is a reasonable procedure if the mesons interact weakly with other hadron-like modes in the thermal bath and the changes in the correlators are small. Large changes will signal the breakdown of this weakly interacting gas picture and there we shall try to compare our observations with the QGP picture.

On a *periodic* lattice the contribution of a pole in the mesonic spectral function to the t-propagator is $\cosh(m(t-N_\tau/2))$ (this m is therefore called "pole-mass"). A broad structure or the admixture of excited states leads to a superposition of such terms. Fitting a given t-propagator by $\cosh(m(t)(t-N_\tau/2))$ at pairs of points $t, t+1$ defines an "effective mass" $m(t)$ which is constant if the spectral function has only one, narrow peak. We shall simply speak about $m(t)$ as "mass": it connects directly to the (pole) mass of the mesons below T_c, while above T_c it will help analyse the dominant low energy structure in the frame of our strategy above. By contrast, we shall speak of "screening mass" ($m^{(\sigma)}$) when extracted from *spatial propagators*. $m^{(\sigma)}$ is different from the $T > 0$ mass (the propagation in the space directions represents a $T = 0$ problem with finite size effects).

To prevent a certain confusion we stress here that we do not look for the eigenstates of the Hamiltonian (transfer matrix), which show up as asymptotic states at $T = 0$. At $T \neq 0$ physics is no longer determined by these pure states but is essentially dependent on the mixtures induced by the thermal bath. For the physical picture and for building models the question is whether these phenomena can be described in terms of some effective excitations, or quasi-particles [6], which "replace" the ground state particle modes. By this we mean, as usual, that the description becomes simpler in terms of these effective modes and therefore it makes sense to use them as long as they appear as quasi-particles, i.e. as not too wide resonances. More illustrating discussion on this point was given in [1].

We use lattices of $12^3 \times N_\tau$ with $N_\tau = 72, 20, 16$ and 12 at $\beta = 5.68$, $\gamma_G = 4$. The renormalised anisotropy is determined at T=0 as $\xi \simeq 5.3(1)$. We find [5] T_c at N_τ slightly above 18, which fixes for the above lattices $T \simeq 0, 0.93T_c, 1.15T_c$ and $1.5T_c$ and $a_\tau \sim 0.044$ fm $= (4.5\ \mathrm{GeV})^{-1}$. The *temporal* and *spatial* correlators are measured for 3 quark masses, and extrapolated to the chiral limit. The various parameters are given in the Table. At each temperature, 60 configurations are used for the analyses of meson correlators (details can be found in [1]). We use periodic (anti-periodic) boundary conditions in the spatial (temporal) directions and gauge-fix to Coulomb gauge. We investigate correlators of the form:

$$G_M(x,t) = \sum_{\mathbf{z},\mathbf{y_1},\mathbf{y_2}} w_1(\mathbf{y_1}) w_2(\mathbf{y_2}) \times \langle \mathrm{Tr}[S(\mathbf{y_1},0;\mathbf{z},t)\gamma_M\gamma_5 S^\dagger(\mathbf{y_2},0;\mathbf{z}+\mathbf{x},t)\gamma_5\gamma_M^\dagger]\rangle \quad (4)$$

$$w_{1,2}(\mathbf{y}) \sim \begin{cases} \delta(\mathbf{y}) & (point) \\ \exp(-ay^p) & (exp.) \end{cases} \quad (5)$$

with S the quark propagator and $\gamma_M = \{\gamma_5, \gamma_1, 1, \gamma_1\gamma_5\}$ for $M = \{Ps, V, S, A\}$ (pseudoscalar, vector, scalar and axial-vector, respectively). We use point and smeared (exponential) *quark* sources and point sink. We fix the exponential (*exp*) source taking the parameters a, p in (5) from the observed dependence on $\mathbf{x}$ of the tempo-

Table 1
Simulation parameters used at every T and meson masses at $T \simeq 0$ (in units a_τ^{-1}). The source parameters a, p in eq. (5) are extracted from the $T \simeq 0$ wave function.

κ_σ	γ_F	m_{Ps}	m_V	a	p
0.081	4.05	0.178(1)	0.196(1)	0.379	1.289
0.084	3.89	0.149(1)	0.175(1)	0.380	1.277
0.086	3.78	0.134(1)	0.164(1)	0.380	1.263

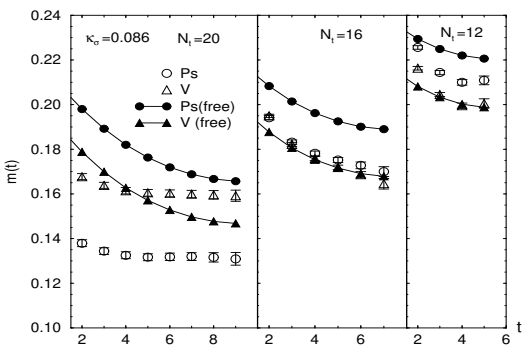

Figure 1. From left to right, effective mass $m(t)$ in units of a_τ^{-1} at $T \simeq 0.93$, 1.15 and $1.5T_c$ (open symbols) vs t, at $\kappa_\sigma = 0.086$. Also shown are the effective masses from the same correlators calculated using free quarks.

ral Ps correlator with *point-point* source at $T \simeq 0$ (see Table). The results of a variational analysis using *point-point*, *point-exp* and *exp-exp* sources indicate that the latter ansatz projects most efficiently onto the ground state at $T = 0$. Therefore we use throughout the *exp-exp* sources for defining hadron operators at high T, according to our strategy.

Note that in agreement with the remarks in the previous paragraphs the source dependence has various origins. At fixed physical distance, say, $ta_\tau = 5a_\tau$, we find a variation in $m(t)$ between *point-exp*, *exp-exp* and *wall* source of $\sim 20\%$ below T_c and $\sim 25\%$ above T_c. This source dependence disappears exponentially with t at low T. By choosing an optimal source, we try to minimise that part of the $m(t)$ variation which is present at $T = 0$. The remaining source dependence includes the genuine physical effects we are looking for, e.g. the width of the dominant low energy contribution. Using the source tuned at $T = 0$ implies the assumption that the spatial structure corresponding to this contribution changes little with T, which allows for a consistency check. There may be, however, also other effects, increasing the uncertainty of the analysis at high T.

We shall now present the results. All masses are given in units a_τ^{-1}, i.e. we plot $mass \times a_\tau$. Errors are statistical only.

a) Effective masses. In Fig. 1 we show the effective mass $m(t)$ of the Ps and V time-propagators at $T \simeq 0.93T_c$, $1.15T_c$ and $1.5T_c$. We notice practically no change from $T = 0$ to $0.93T_c$, while above T_c clear changes develop: $m(t)$ depends strongly on t, it increases significantly, and the Ps and V reverse their positions. Because of the large changes at high T we compare here with the unbound quark picture of the high T regime of QGP. For this we calculate mesonic correlators using, with the same source, free quark propagators S_0 instead of S in (4), with $\gamma_F = \xi = 5.3$, and assuming a thermal mass for the quarks: $m_q^{\rm thermal} \approx g^2T/\sqrt{6} \sim 0.036 a_\tau^{-1} T/T_c$, tuned to give a good agreement with the measured rho channel above T_c. Similarities are apparent - see Fig. 1. Generally above T_c, $m(t)$ shows stronger t-dependence, which means that the spectral function selected by the *exp-exp* source no longer has just one, narrow contribution, as for $T < T_c$.

b) Wave functions. We have also analysed the "wave functions", i.e. the behaviour of the temporal correlators with the quark-antiquark distance at the sink. In Fig. 2 we compare the Ps wave functions normalised at $x = 0$, $G_{Ps}(x,t)/G_{Ps}(0,t)$, at several t for $T \simeq 0.93T_c$ (which is very similar to $T \simeq 0$) and $T \simeq 1.5T_c$ at our lightest quark mass ($\kappa_\sigma = 0.086$) and for the free quark case. Our *exp-exp* source appears somewhat too broad at $T \simeq 0.93T_c$: the quarks go nearer each other while propagating in t. Interestingly enough, this is also the case at $T \simeq 1.5T_c$: the spatial distribution shrinks and stabilises, indicating that even at this high temperature there is a tendency for quark and antiquark to stay together. This is in clear contrast to the free quark case which never shows such a behaviour regardless of the source (in Fig. 2 we use the *exp-exp* source). Hence the only effect of

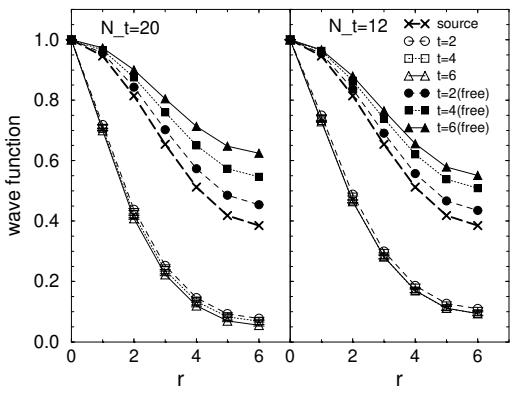

Figure 2. Ps wave functions ($\kappa_\sigma = 0.086$, *exp-exp* source) normalised at $r = 0$ vs quark separation r at $t = 2, 4$ and 6, using full and free propagators. Also plotted is the initial distribution of separations as given by the source, $\int d^3y w(\mathbf{y}+\mathbf{r})w(\mathbf{y})$. $T \simeq 0.93T_c$ (left) and $T \simeq 1.5T_c$ (right).

the temperature on the wave function is to make it slightly broader. The same holds also for the other mesons at all quark masses.

c) Masses and screening masses. We fit the Ps, V, S and A time-correlators to single hyperbolic functions at the largest 3 t-values. For the S-meson we only use the connected correlator. *Above T_c we assume that these masses characterise the dominant low energy structure selected by our source* (e.g., the putative, unstable states described by the wave functions discussed above). We also extract screening masses from spatial correlators at the largest 3 x. Since the spatial physical distance is large we use *point-point* source for all T (a gauge invariant extended source leads to similar results). The results for m and $m^{(\sigma)}$ at $\kappa_\sigma = 0.086$ are shown in Fig. 3 (above T_c, m and, to a smaller extent, also $m^{(\sigma)}$ may be overestimated). We extrapolate m and $m^{(\sigma)}$ in $1/\kappa = 2m_0 + 8$ to the chiral limit from the 3 quark masses analysed. We assume that the Ps extrapolates in mass squared for $T < T_c$. Above T_c the κ dependence is very weak. Up to T_c screening masses and masses remain similar, while above T_c the former become much larger than the latter, both at finite quark mass and in the chiral limit – see Fig. 3 [7]. In the high T regime of QGP

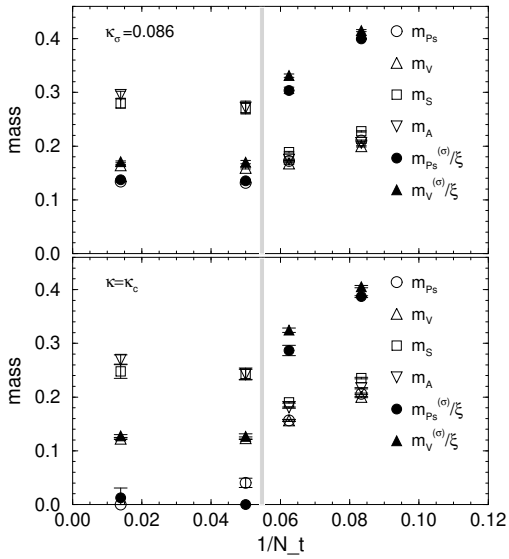

Figure 3. Temperature dependence of the mass m (open symbols) and screening mass $m^{(\sigma)}$ (full symbols) in units a_τ^{-1}, for $\kappa_\sigma = 0.086$ (upper plot) and in the chiral limit (lower plot). The vertical gray lines indicate T_c. The data correspond to $T \simeq 0,\ 0.93T_c,\ 1.15T_c$ and $1.5T_c$.

one expects $m^{(\sigma)} \sim 2\pi/N_\tau \sim 0.4(0.5)$ in units of a_τ^{-1} for $T \simeq 1.15T_c(1.5T_c)$, respectively, to be compared with the values in Fig. 3 of $\sim 0.3(0.4)$.

In conclusion, in this quenched QCD analysis the changes of the meson properties with temperature appear to be small below T_c, while above T_c they become important and rapid, but not abrupt. Here we observe apparently opposing features: On the one hand, the behaviour of the propagators, in particular the change in the ordering of the mass splittings could be accounted for by free quark propagation [2] in the mesonic channels above T_c, which would also explain the variation of $m(t)$. On the other hand, the behaviour of the wave functions obtained from the 4-point correlators suggests that there can be low energy excitations in the mesonic channels above T_c, remnants of the mesons below T_c. They would

[2]We mean S_0 with some effective m_q induced by the interaction. The larger $m(t)$ in Ps channel as compared with V is a peculiarity of the free Wilson quarks (3). Its counterpart for staggered fermions is an oscillating behaviour, quoted in [9] also as indicator of free quark propagation.

be characterised by a mass giving the location of the corresponding bump in the spectral function. The variation of $m(t)$ with t and with the source would then indicate a resonance width increasing with T, although it may simply reflect the uncertainty in our treatment of the low energy states. We remark that using free quark propagators the source dependence is much stronger. Remember that our source is not chosen arbitrarily but such as to reproduce a "pure" meson source at $T = 0$; at high T, however, it may allow admixture of other contributions, and m becomes increasingly ambiguous. We see chiral symmetry restoration above T_c both in the masses and in the screening masses, with the latter increasing faster than the former and remaining below the free gas limit at $T \simeq 1.5T_c$. The exact amount of splitting among the channels and the precise ratio between m and $m^{(\sigma)}$ may, however, be affected also by uncertainties in our ξ calibration. Finally, note that this is a quenched simulation, with incomplete dynamics. This may, however, have an interesting consequence: since there is no pair creation here we cannot have "standard " string breaking *hadron* $\rightarrow$ 2 *hadrons*. A genuine widening of the mesonic spectral function can therefore only come from the decay *meson* $\rightarrow q + \bar{q}$. In full QCD these two effects would be superposed, in quenched QCD a signal for widening of the spectral function implies the existence of strongly interacting but unbound $q\bar{q}$ states, coexisting with meta-stable mesons.

A possible physical picture is therefore this: Mesonic excitations subsist above T_c (up to at least $1.5T_c$) as unstable modes (resonances), in interaction with unbound quarks and gluons. Our results are consistent with this, but there may be also other possibilities (cf [8,9], cf [4] and references therein). E.g., in a study of meson propagators including dynamical quarks but without wave function information [9], one found masses and (spatial) screening masses $\propto T$ above T_c and indication for QGP with "deconfined, but strongly interacting quarks and gluons". The complex, non-perturbative structure of QGP (already indicated by equation of state studies up to far above T_c [10]) is also confirmed by our analysis of general mesonic correlators. From our study however, the detailed low energy structure of the mesonic channels appears to present further interesting, yet unsolved aspects. Further work is needed to remove the uncertainties still affecting our analysis. This concerns particularly the ξ calibration and the question of the definition of hadron operators at high T, which appear to have been the major deficiencies, besides the smaller lattices, affecting earlier results [11]. We shall also try to extract information directly about the spectral functions [12].

Acknowledgements: We thank JSPS, DFG and the European Network "Finite Temperature Phase Transitions in Particle Physics" for support. The calculations were done on AP1000 at Fujitsu Parallel Comp. Res. Facilities and Intel Paragon at INSAM, Hiroshima Univ.

REFERENCES

1. QCD-TARO Collaboration (Ph. de Forcrand *et al.*), Phys. Rev. D **63** (2001) 054501.
2. J. Engels, F. Karsch and H. Satz, Nucl. Phys. **B205**[FS5] (1982) 239.
3. F. Karsch, Nucl. Phys. **B205**[FS5] (1982) 285.
4. H. Meyer-Ortmanns, Rev. Mod. Phys. **68** (1996) 473; H. Satz, hep-ph/9706342.
5. From the peak of the Polyakov loop susceptibility; see QCD-TARO: M. Fujisaki et al., Nucl. Phys. B (Proc.Suppl.) **53** (1997) 426.
6. H. Narnhofer, M. Requardt and W. Thirring, Commun. Math. Phys. **92** (1983) 247.
7. A similar behaviour is obtained in T. Hatsuda and T. Kunihiro, Phys. Rep. **247** (1994) 221 from an NJL effective model; an increasing m_π is also obtained in J. Berges, D.U. Jungnickel and C. Wetterich, hep-ph/9705474.
8. C. DeTar and J. Kogut, Phys. Rev. D **36** (1987) 2828; C. DeTar, Phys. Rev. D **37** (1988) 2328.
9. G. Boyd, S. Gupta, F. Karsch, E. Laermann, Z. f. Physik C **64** (1994) 331.
10. G. Boyd et al., Nucl. Phys. **B469** (1996) 419.
11. T. Hashimoto, A. Nakamura and I.-O. Stamatescu, Nucl. Phys. **B400** (1993) 267.
12. QCD-TARO: Ph. de Forcrand et al., Nucl. Phys. B (Proc.Suppl.) **63** (1998) 460.